Photosynthesis Research (2018) 138:57–71
https://doi.org/10.1007/s11120-018-0539-3

ORIGINAL ARTICLE

Comparison of photosynthetic performances of marine picocyanobacteria with different configurations of the oxygen-evolving complex

Frédéric Partensky[1,2] · Daniella Mella-Flores[1,2,3,4] · Christophe Six[1,2] · Laurence Garczarek[1,2] · Mirjam Czjzek[1,5] · Dominique Marie[1,2] · Eva Kotabová[6] · Kristina Felcmanová[6,7] · Ondřej Prášil[6,7]

Received: 16 March 2018 / Accepted: 20 June 2018 / Published online: 25 June 2018

Abstract

The extrinsic PsbU and PsbV proteins are known to play a critical role in stabilizing the Mn_4CaO_5 cluster of the PSII oxygen-evolving complex (OEC). However, most isolates of the marine cyanobacterium *Prochlorococcus* naturally miss these proteins, even though they have kept the main OEC protein, PsbO. A structural homology model of the PSII of such a natural deletion mutant strain (*P. marinus* MED4) did not reveal any obvious compensation mechanism for this lack. To assess the physiological consequences of this unusual OEC, we compared oxygen evolution between *Prochlorococcus* strains missing *psbU* and *psbV* (PCC 9511 and SS120) and two marine strains possessing these genes (*Prochlorococcus* sp. MIT9313 and *Synechococcus* sp. WH7803). While the low light-adapted strain SS120 exhibited the lowest maximal O_2 evolution rates (P_{max} per divinyl-chlorophyll *a*, per cell or per photosystem II) of all four strains, the high light-adapted strain PCC 9511 displayed even higher P^{Chl}_{max} and P^{PSII}_{max} at high irradiance than *Synechococcus* sp. WH7803. Furthermore, thermoluminescence glow curves did not show any alteration in the B-band shape or peak position that could be related to the lack of these extrinsic proteins. This suggests an efficient functional adaptation of the OEC in these natural deletion mutants, in which PsbO alone is seemingly sufficient to ensure proper oxygen evolution. Our study also showed that *Prochlorococcus* strains exhibit negative net O_2 evolution rates at the low irradiances encountered in minimum oxygen zones, possibly explaining the very low O_2 concentrations measured in these environments, where *Prochlorococcus* is the dominant oxyphototroph.

Keywords Marine cyanobacteria · *Prochlorococcus* · *Synechococcus* · Photoacclimation · Photosystem II · Oxygen-evolving complex · Oxygen minimum zones

Introduction

The chlorophyll biomass of warm, open ocean ecosystems is largely dominated by tiny photosynthetic cells (< 2–3 µm), collectively called the 'picophytoplankton' (Stockner 1988). In vast oceanic areas, up to 99% of the oxyphototrophic cells constituting this size fraction are cyanobacteria, a group largely dominated by the *Prochlorococcus* and *Synechococcus* genera (Campbell and Vaulot 1993; Campbell et al. 1994). Together these two photosynthetic prokaryotes are thought to contribute for 32 to 80% of primary production in oligotrophic areas (Li et al. 1992; Li 1994; Liu et al. 1997) and up to 25% of the global marine primary productivity (Flombaum et al. 2013).

Because of their ecological importance and tiny sizes (about 1 and 0.6 µm equivalent cell diameters, respectively), *Prochlorococcus* and *Synechococcus* have been privileged targets for genome sequencing and numerous complete genomes are now available for each genus, representing a large spectrum of genetic diversity, physiological types and ecological niches (Kettler et al. 2007; Dufresne et al. 2008; Scanlan et al. 2009; Biller et al. 2014). The comparison of *Prochlorococcus* genomes has revealed that a dramatic reduction of genome size and G + C content has affected

Frédéric Partensky and Daniella Mella-Flores have contributed equally to this paper

Electronic supplementary material The online version of this article (https://doi.org/10.1007/s11120-018-0539-3) contains supplementary material, which is available to authorized users.

✉ Frédéric Partensky
frederic.partensky@sb-roscoff.fr

Extended author information available on the last page of the article

many lineages in this genus, including most low light-adapted (LL) and all high light-adapted (HL) clades (Rocap et al. 2003; Dufresne et al. 2005; Partensky and Garczarek 2010; Batut et al. 2014). For instance, the HLI strain MED4 has one of the smallest genomes known so far for an oxyphototroph (1.66 Mbp) and a very low G + C content (30.8%) and comparable genome characteristics were found in the LLII strain SS120 (1.75 Mbp; G + C% = 36.4%). In contrast, strain MIT9313, a member of the LLIV clade located at the base of the *Prochlorococcus* radiation, has a genome size (2.41 Mbp) and G + C content (50.7%) more similar to marine *Synechococcus* spp. (genome size ranging from 2.2 to 3.0 Mbp and G + C% between 52.5–66.0%; Dufresne et al. 2008; Scanlan et al. 2009). Thus, genome streamlining seemingly occurred after the differentiation of the *Prochlorococcus* genus from its common ancestor with marine *Synechococcus* spp. (Dufresne et al. 2005). This process was accompanied by a reduction of cell size and individual cell components, such as carboxysomes, photosynthetic membranes or even the cell wall (Ting et al. 2007) and likely plays a critical role in the fitness of *Prochlorococcus* to oligotrophic environments (Dufresne et al. 2008; Partensky and Garczarek 2010).

When compared to marine *Synechococcus*, all *Prochlorococcus* strains with a streamlined genome lack a number of genes, such as those encoding glycolate oxidase or an ABC transporter involved in the uptake of the compatible solute glucosylglycerol (Scanlan et al. 2009; Partensky and Garczarek 2010). Most genes encoding phycobilisomes, a type of light-harvesting complexes found in most cyanobacteria including all marine *Synechococcus* spp., have been also lost in *Prochlorococcus* spp.—apart from some phycoerythrin remnants (Hess et al. 1996)—and the major photosynthetic antenna in the latter genus is therefore constituted of membrane-intrinsic Chl-binding proteins, termed Pcb (Partensky and Garczarek 2003) or CBP (Chen et al. 2008). Although most other photosynthetic genes have been retained and are generally well conserved in *Prochlorococcus*, all strains with streamlined genomes lack *psb32*, coding for a protein thought to protect photosystem II (PSII) from photodamage and to accelerate its repair (Wegener et al. 2011), as well as *psbU* and *psbV*, encoding two small extrinsic proteins of the oxygen-evolving complex (OEC; De Las Rivas et al. 2004).

The OEC is the part of the PSII where the water-splitting reaction takes place at the level of the Mn_4CaO_5 cluster (hereafter Mn cluster; Kawakami et al. 2011). According to the structure of *Thermosynechococcus elongatus* PSII, PsbU (a.k.a. PSII 12 kDa extrinsic protein) and PsbV (a.k.a. cytochrome c_{550}) together with the main OEC protein PsbO form a large protein cap in the lumenal side of PSII that shields the Mn cluster from the bulk aqueous phase (Zouni et al. 2001; Ferreira et al. 2004; Guskov et al. 2009). This structural organization is consistent with a role of these extrinsic proteins in stabilizing PSII. Indeed, it has been reported that deletion of PsbU and PsbV proteins may affect PSII stability in several ways. In *Synechocystis* sp. PCC 6803, *psbV*-less mutants were unable to grow in the absence of Ca^{2+} and Cl^-, while cyanobacterial and red algal *psbU*-less mutants showed a decreased growth in the same condition, suggesting that these genes help in maintaining the proper ion environment for oxygen evolution, presumably by acting in the affinity of PSII for Ca^{2+} and Cl^- (Shen et al. 1997; Enami et al. 2000; Okumura et al. 2001, 2007; Inoue-Kashino et al. 2005). Additionally, these deletion mutants exhibited a drop of oxygen evolution (a 40% and 81% decrease in *Synechocystis* sp. PCC 6803 *psbV*- and *psbU*-less mutants, respectively; Shen et al. 1995, 1997) concomitant with a destabilization of PSII complex, as manifested by the decreased proportion of assembled PSII centres in *psbV*-less mutants (Shen et al. 1995, 1997; Kimura et al. 2002) and the impairment of the donor side of PSII in mutants lacking *psbU* (Inoue-Kashino et al. 2005). It has also been reported that the presence of PsbU and PsbV protects PSII against dark inactivation (Shen et al. 1998; Veerman et al. 2005) and contributes to the thermal stability of the OEC function (Nishiyama et al. 1997, 1999). Moreover, PsbU was shown to protect PSII against photodamage (Inoue-Kashino et al. 2005) and oxidative stress (Balint et al. 2006).

Considering the critical roles that PsbU and PsbV are thought to play in cyanobacterial OEC, one may wonder whether the loss of these genes in all *Prochlorococcus* lineages except members of the LLIV clade has consequences on the ability of these natural mutants to evolve oxygen. Here, oxygen evolution was compared at several growth irradiances between two *Prochlorococcus* strains lacking *psbU* and *psbV* (*P. marinus* SS120 and PCC 9511) and two marine picocyanobacterial strains that have retained these genes (*Prochlorococcus* sp. MIT9313 and *Synechococcus* spp. WH7803). Structural homology modelling of the PSII of MED4 (a strain very closely related to PCC 9511; Rippka et al. 2000) was also used to look for possible compensation mechanism such as extension of other PSII subunits.

Materials and methods

Strains and culture condition

The four clonal picocyanobacterial strains used in this study were retrieved either from the Roscoff Culture Collection (http://roscoff-culture-collection.org/) or the Pasteur Culture Collection (cyanobacteria.web.pasteur.fr/). *Prochlorococcus* sp. MIT9313 (RCC407), *P. marinus* PCC 9511, *P. marinus* SS120 (RCC156) and *Synechococcus* sp. WH7803 (RCC752) were grown at 22 °C in 0.2 µm filtered PCR-S11 medium (Rippka et al. 2000) supplemented with

1 mM $NaNO_3$ (nitrates are used only by WH7803) under continuous light provided by Sylvania Daylight 58W/154 fluorescent neon tubes. Cultures were acclimated for > 30 generations at several irradiances (see results) and diluted 2–3 days prior to measurements of Photosynthesis vs. Irradiance (P–E) curves, to ensure that cultures were in early to mid-exponential phase and exhibited a balanced growth (Brand et al. 1981) and optimal photosynthetic performances (Glibert et al. 1986). The physiological status of cultures was monitored just prior to experiments by measuring the PSII fluorescence quantum yield (F_V/F_M) using a Pulse Amplitude Modulated (PAM) fluorometer (PhytoPAM, Walz, Effeltrich, Germany), as previously described (Six et al. 2007; Garczarek et al. 2008) and no samples with F_V/F_M lower than 0.43 were retained for the experiment (mean $F_V/F_M = 0.58 \pm 0.07$; $n = 22$). For oxygen evolution analysis, exponentially growing cultures were concentrated between 10- and 20-fold by gentle centrifugation at 3900×*g* for *Synechococcus* cells and 5450×*g* for *Prochlorococcus* for 7 min at 22 °C, using an Eppendorf 5804R centrifuge (Hamburg, Germany) and aliquots were taken from the concentrate for flow cytometry, chlorophyll assays and immunoblotting. Each experiment was replicated four to six times.

Gene expression

In order to check for the expression of *psbO* and, when present, *psbU* and *psbV* genes in the different strains, an independent set of cultures was performed under the standard LL culture conditions (18 µmol photons m^{-2} s^{-1}). A 150 mL volume was sampled from each culture strain, immediately cooled down to about 2–4 °C by swirling the sample in liquid nitrogen and harvested by centrifugation (7 min at 4 °C, 17,700×*g*, Eppendorf 5804R) in the presence of 0.03% (v/v) of pluronic acid (Sigma-Aldrich). Cell pellets were then resuspended in 300 µL Trizol (Invitrogen, Carlsbad, CA), frozen in liquid nitrogen and stored at − 80 °C until extraction. Frozen cells in Trizol were then thawed for 15 min in a water bath set at 65 °C with regular vortexing. This step was followed by two chloroform extractions (0.2 mL of chloroform per mL of Trizol) before purification using the miRNeasy kit (Qiagen, Valencia, CA). A DNase treatment (DNAse I FPLC purified, GE Healthcare Bio-Sciences, Uppsala, Sweden) was performed for 30 min at room temperature. Purified RNAs were eluted in 35 µL of RNase-free water and stored at − 80 °C. Primers for reverse transcription and real-time PCR (RT-PCR) were designed using Primer Express (Applied Biosystem, v2.0; Online Resource_Table_S1). The cDNA was obtained by reverse transcription of 100 ng of RNA and 8 pmol of the reverse primer. RNA was denatured for 10 min at 70 °C in the presence of 20 U of RNase inhibitor (RNasine, Ambion, Austin, TX) before addition of a mix of SuperScriptII (Life Technologies Inc. Gibco-BRL, Grand Island, NY), 5X reaction buffer, 2 µM DTT and 0.25 mM of each dNTP. The reaction mix was incubated at 42 °C for 50 min followed by 15 min of cDNA denaturation at 72 °C. RT-PCR was done on a Biosystem GeneAmp 5700 (Life Technologies Inc., Applied Biosystems, Foster City, CA) using the SYBR Green PCR master mix (Applied Biosystem). Real-time PCRs were performed with the GeneAmp 5700 detection system (Perkin Elmer, Waltham, MA) using the SYBR Green PCR master mix (Applied Biosystems) on a 1:50th diluted cDNA in the presence of 300 nM primers. The PCR reaction program consisted of a sequence of 10 min at 95 °C followed by 40 cycles of 15 s at 95 °C and 1 min at 60 °C.

Oxygen evolution

Photosynthetic oxygen evolution was measured using a Neofox system equipped with an oxygen optode connected to an optical fiber (Ocean Optics Inc., Dunedin, FL). Measurements were carried out on 2 mL aliquots of concentrated cultures placed into a cuvette, homogenized with a magnetic stirrer and maintained at 22 °C by circulation of thermostated water from a MultiTempIII temperature-controlled bath (GE Healthcare, Amersham Biosciences, Uppsala, Sweden). The temperature probe coupled with the Neofox system was also maintained at 22 °C in the same bath. Pilot measurements allowed us to check that oxygen rates were not modified by addition of 2 mM $NaHCO_3$, so they were not limited by availability of inorganic carbon. P–E curves were derived from measured rates of O_2 evolution obtained by exposing cells to a range of increasing actinic light levels, obtained using a KL 1500 LCD halogen light source (Schott, Mainz, Germany). Each illumination period (5–10 min) was followed by a comparable dark period used to measure respiration (see a representative experiment in Online Resource_Fig_S1). Oxygen-evolving rates (µmol O_2 mg Chl^{-1} h^{-1}) were determined by fitting P–E curves using the dynamic fit function of Sigmaplot (Systat Softwares, San Jose, CA) with the following equation (Platt and Jassby 1976):

$$P^x = P^x{}_m \cdot \tanh\left(\alpha^x \cdot E / P^x{}_m\right) - R^x, \quad (1)$$

where P^x is the net rate of oxygen evolution at an irradiance E (µmol photon m^{-2} s^{-1}), $P^X{}_m$ is the maximal, light-saturated oxygen evolution rate, α^x is the initial light-limited slope of the P–E curve and R^x is the dark respiration rate. The x stands for the parameter used to normalize the data, i.e. (DV−) Chl *a*, cell or mole D2 (see below). The saturating irradiance E_k (µmol photon m^{-2} s^{-1}) was calculated using the equation:

$$E_k = P^{Chl}{}_m / \alpha^{Chl} \quad (2)$$

and the compensation irradiance was determined as follows (Geider and Osborne 1992):

$$E_0 = R^{Chl} / \alpha^{Chl}. \quad (3)$$

Chlorophyll assays

Chlorophyll (Chl) concentrations were determined after extracting pigments in 100% cold methanol using a spectrophotometer UV − mc² (SAFAS, Monaco). For *Synechococcus*, Chl *a* concentrations were assessed using Chl *a* extinction coefficient (Roy et al. 2011). For *Prochlorococcus* strains, which contain unique divinyl derivatives of both Chl *a* and *b* (hereafter DV-Chl *a* and b; Goericke and Repeta 1992), concentrations were assessed using the equations of Porra (2002) for methanol, which we modified using the absorption values at the red peak of DV-Chl *a* (instead of A_{665} for Chl *a*) and 13 nm before the red peak for DV-Chl *b* (instead of A_{652} for Chl *b* in Porra's equation).

Flow cytometry

A 10 µL aliquot from each concentrated culture was diluted in 990 µL of fresh PCR-S11 medium in the presence of 0.25% glutaraldehyde grade II (Sigma- Aldrich, St Louis, MO, USA) for 20 min in the dark at room temperature, then flash frozen in liquid nitrogen and stored at -80 °C until analysis. Cyanobacterial concentration in cultures was determined using a BD FACS Canto flow cytometer (Becton Dickinson, San Jose, CA, USA), as previously described (Marie et al. 1999). Heterotrophic bacteria were also counted after DNA staining using SYBR Green (Marie et al. 1999) in order to check that contamination was minimal (always < 20% total cell counts) during oxygen measurements.

Quantitation of core photosystem proteins

In order to normalize the oxygen production per photosystem, we quantified the relative amounts of the D2 subunit of photosystem II, essentially as described by Pittera et al. (2014), except that they quantified D1. Briefly, cell pellets were resuspended in an extraction buffer and lysed, the total protein concentration was determined, then samples were denatured for 2 min at 80 °C in the presence of 50 mM dithiothreitol and loaded on a 4–12% acrylamide precast NuPAGE mini-gel (Invitrogen) along with D2 protein standards (Agrisera, Sweden), used to draw the calibration standard curve. After gel electrophoresis, proteins were transferred onto a methanol prehydrated polyvinylidene di-fluoride (PVDF) membrane (Sigma-Aldrich) for 70 min at 30 mA for two membranes, and then immediately immersed in Tween 20-tris-buffered saline (Tween-TBS; Sigma-Aldrich) buffer pH 7.6 (0.1% Tween 20, 350 mM sodium chloride, 20 mM Trizma base) containing 2% (w:vol) blocking agent (Amersham Biosciences) overnight at 4 °C. The primary antibody PsbD (photosystem II D2 core subunit; Agrisera, Sweden) was diluted at 1:50,000 in Tween-TBS in the presence of 2% blocking agent and the membrane was soaked in this solution for 1 h with slow agitation at room temperature. After discarding the primary antibody solution and extensive washing in Tween-TBS, the anti-rabbit secondary antibody coupled to horseradish peroxidase (Biorad) diluted at 1:50,000 in Tween-TBS buffer containing 2% blocking agent was added for 1 h. The membrane was washed three times for 5 min in Tween-TBS buffer prior to revelation using an enhanced chemiluminescence reagent (ECL, Amersham Biosciences). Signals were measured using the ImageQuant software (GE Healthcare, Bio-Sciences, Uppsala, Sweden; for example western blots, see Online Resource_Fig_S2). Protein concentrations were determined by fitting the sample signal values on the recombinant D2 protein standard curve. Pilot experiments were performed to ensure that sample signals fell within the range spanned by the standard curve.

Thermoluminescence

Thermoluminescence (TL) glow curves were recorded using a TL 200/PMT instrument (Photon Systems Instruments, Drasov, Czech Republic), as described by Belgio et al. (2018). For each cyanobacterial strain studied, we first determined the volume of sample that provided linear response in terms of thermoluminescence (TL) intensity (usually 2–6 mL of culture). After sample collection, the determined volume of cell suspension was filtered through a Pragopor #6 nitrocellulose membrane filter (pore size: 0.4 µm; Pragochema, Czech Republic) and placed onto the sample holder. Samples were cooled down to 3 °C, where series of 1–5 saturating single turnover flashes (50 µs, 200 ms apart) were given 1 s prior to the start of the heating and recording phase. TL curves were then recorded from 3 to 65 °C with a heating rate of 0.5 °C s^{-1}. For all TL measurements reported here, the sensitivity of the TL detection system was kept the same in order to allow quantitative comparisons among studied strains. For the measurements in the presence of 10 µM DCMU, the inhibitor was added to suspension before filtering and the sample was cooled down to − 10 °C. TL was then measured from − 10 to 65 °C.

3D modelling of *P. marinus* MED4 PSII

The 3D structure of the whole PSII of *P. marinus* MED4 was performed using the MODELLER software (Eswar et al. 2007), based on sequence homologies with PSII proteins from *Thermosynechococcus elongatus* BP-1, for which the crystallographic structure was resolved at 2.9 Å (PDB access code: 3BZ1 and 3BZ2; Guskov et al. 2009). First, sequences of each PSII subunit of *T. elongatus* and *P. marinus* were

aligned using clustalW (Thompson et al. 1994). Alignments combined with the atomic coordinates of each subunit of *T. elongatus* in the 3D structure were used as entries for MODELLER (Webb and Sali 2014). Ten models were calculated for each subunit from *P. marinus* and the best model was assessed using the 'objective function' parameter of the MODELLER software. The best model for each subunit was then superimposed to the crystallographic structure of the corresponding subunit from *T. elongatus* using TURBO-FRODO (Roussel and Cambillau 1991) in order to reconstitute the whole 3D model of *P. marinus* PSII. The figure was then realized using PYMOL (DeLano 2002).

Results

Transcription of OEC genes

Since *psbU* and *psbV* genes are missing in the genome of *Prochlorococcus* strains MED4 and SS120 (Online Resource_Table_S2), we checked by RT-PCR whether these genes were effectively expressed in *Prochlorococcus* sp. MIT9313, using *Synechococcus* sp. WH7803 as positive control (Table 1). Expression of the core *psbO* gene, encoding the main protein of the OEC, was also measured in all strains. The number of PCR cycles needed to reach the threshold level (i.e. the number of cycles needed to detect a real signal from the samples) was much lower in the experimental sample with reverse transcription (+RT) than in the control (−RT), where it was sometimes too high (> 40) to be detectable (Table 1). These results clearly show that the *psbO* gene was highly expressed in all tested strains in standard culture conditions. Similarly, the large differences between +RT and −RT conditions for both *psbU* and *psbV* genes showed that these genes were strongly expressed in both *Synechococcus* sp. WH7803 and *Prochlorococcus* sp. MIT9313, allowing us to reject the hypothesis that these are pseudogenes in the latter strain, with the caveat that differences in the levels of expression at the mRNA and protein levels are often observed in cyanobacteria (see e.g. Welkie et al. 2014).

Maximal oxygen evolution rates

In order to determine whether the absence of the PsbU and PsbV proteins in the RCII of *Prochlorococcus* strains SS120 and MED4 could affect their oxygen-evolving characteristics compared to strains possessing these proteins, light response curves were determined at three acclimation irradiances (LL = 18 µmol photons m^{-2} s^{-1}; ML = 75 µmol photons m^{-2} s^{-1} and HL = 163 µmol photons m^{-2} s^{-1}) for *P. marinus* PCC 9511 and *Synechococcus* sp. WH7803 strains and only the former two irradiances for the LL-adapted *Prochlorococcus* strains SS120 and MIT9313, which could not grow at the highest irradiance. Given the significant differences in cell size, number of PSII per unit biomass as well as in the nature and composition of the light-harvesting complexes between these four strains (Kana and Glibert 1987a; Moore and Chisholm 1999; Partensky et al. 1993; Six et al. 2007; Ting et al. 2007), P–E curves (Online Resource_Fig_S3–S5) and the corresponding maximal net O_2 evolution rates (P_m) were normalized per (DV-)Chl *a*, per cell and per PSII, in order to ease comparisons (Fig. 1a–c).

Maximal O_2 evolution rates per (DV−)Chl *a* (P^{Chl}_m) globally increased with increasing growth irradiance for all cyanobacterial strains except for MIT9313, which exhibited the highest rate among all three *Prochlorococcus* strains at LL (P^{Chl}_m = 342 mol O_2.[mol DV-Chl *a*]$^{-1}$ h^{-1}) but a lower rate at ML (Fig. 1a and Online Resource_Fig_S3). The record P^{Chl}_m value was observed at HL for PCC 9511 (959 mol O_2.[mol DV-Chl *a*]$^{-1}$.h^{-1}), showing that despite lacking PsbU/V, this strain is a very efficient oxyphototroph and is truly HL-adapted. It is worth noting that at the lowest irradiance tested (18 µmol photons m^{-2} s^{-1}), all picocyanobacterial strains globally consumed more oxygen than they emitted (Fig. 2a).

When rates were normalized per cell (Fig. 1b and Online Resource_Fig_S4), the highest P^{Cell}_m values were, as

Table 1 Expression of genes coding for the oxygen-evolving complex in the four picocyanobacterial strains used in this study

Gene	*P. marinus* PCC 9511		*P. marinus* SS120		*Prochlorococcus* sp. MIT9313		*Synechococcus* sp. WH7803	
	−RT	+RT	−RT	+RT	−RT	+RT	−RT	+RT
psbO	36	25.6	36.2	22.7	n.d.	28.9	n.d.	26.6
psbU	n.a.	n.a.	n.a.	n.a.	37.7	21.6	n.d.	23.2
psbV	n.a.	n.a.	n.a.	n.a.	37.3	23.1	37.5	26.4

Values correspond to the number of cycles needed to reach a fixed fluorescence threshold

Difference in the number of cycles without reverse transcription (-RT), i.e. DNA, and after reverse transcription (+RT), i.e. mRNA, is proportional to the expression level

n.a. not applicable, *n.d.* not detected

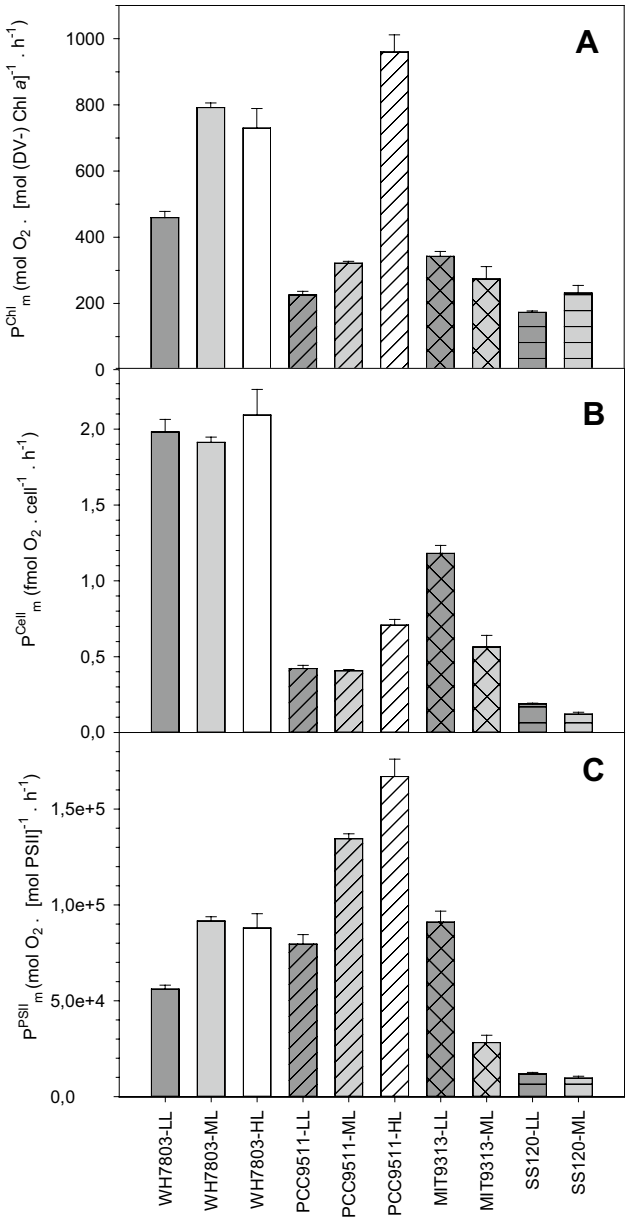

Fig. 1 Comparison of maximal rates of oxygen evolving (P_m) for the four tested marine picocyanobacterial strains grown at low, medium and/or high continuous growth irradiance (LL, 18 ± 3 µmol photons m^{-2} s^{-1}; ML, 75 ± 10 µmol photons m^{-2} s^{-1}; HL, 163 ± 12 µmol photons m^{-2} s^{-1}; the latter irradiance was only applicable for *Synechococcus* sp. WH7803 and *Prochlorococcus marinus* PCC 9511). **a** Values normalized per total Chl, i.e. Chl *a* only for *Synechococcus* sp. WH7803 and the sum of DV-Chl *a* and *b* for *Prochlorococcus* strains MED4, SS120 and MIT9313. **b** Values normalized per cell. **c** Values normalized per PSII (D2 protein). All measurements are average ± SD of 4 to 6 biological replicates

expected, observed for the two strains exhibiting the largest cell sizes, i.e. WH7803 and MIT9313 (Kana and Glibert 1987a; Ting et al. 2007). PCC 9511 was the sole strain for which P^{Cell}_m significantly increased with irradiance, while it dropped twofold between LL and ML for MIT9313.

When rates were normalized per PSII complex (Fig. 1c and Online Resource_Fig_S5), PCC 9511 exhibited the highest P^{PSII}_m value at both ML and HL with a regular increase between LL and HL, while for MIT9313 P^{PSII}_m was threefold lower at ML than LL. It is worth noting that the proportion of PSII per total protein tended to decrease with increasing growth irradiance (I_g) in the two HL-adapted strains (WH7803 and PCC 9511), while it was virtually unchanged between LL and ML in the two LL-adapted strains (Fig. 3). With the caveat that cultures exhibited a limited contamination by heterotrophic bacteria that could somewhat bias the measured amount of total proteins, the much lower maximal evolution rates per PSII measured for *P. marinus* SS120 compared to the two other *Prochlorococcus* strains (Fig. 1c) might be explained in part by the fact that the latter strain seemingly contains a particularly high number of PSII per total protein (Fig. 3), although the reason why its rates were also very low when normalized per cell (Fig. 1b) remains unclear. Altogether, our data suggest that (i) HL-adapted strains mainly acclimate to increasing I_g by reducing their total PSII number, whereas LL-adapted strains rather reduce the size of their PSII antennae and (ii) the PSII efficiency is much less affected by increases in I_g in HL- than in LL-adapted strains.

Other photosynthetic parameters

The low light capture efficiency per cell, as assessed by the initial light-limited slope of the P–E curve (α^{Cell}; Fig. 2b), was expectedly higher for the larger cell-sized strains, *Synechococcus* sp. W7803 and *Prochlorococcus* sp. MIT 9313. α^{Cell} tended to decrease between LL and ML in all strains, as a likely result from a decrease of the antenna size, but this trend was statistically significant only in the LL-adapted strain MIT9313.

The HL-adapted strains *Synechococcus* sp. WH7803 and *P. marinus* PCC 9511 displayed slightly higher saturation irradiances at LL (E_k > 150 µmol photons m^{-2} s^{-1}; Fig. 2c) than the LL-adapted strains MIT9313 and SS120 (< 150 µmol photons m^{-2} s^{-1}), but while E_k increased with irradiance in the former strains, it slightly decreased in the latter strains. The compensation irradiance (E_0) occurred at about one-fourth (26.4 ± 4.5%) of the E_k values in all strains (Fig. 2d).

Thermoluminescence

TL glow curves in the temperature range 10–50 °C result from thermally induced radiative back reactions within PSII, namely from the $S_{2/3}Q_B^-$ charge recombination (Rutherford et al. 1984). We measured the shapes and intensities of the TL glow curves of strains grown at LL in order to compare the energetics of the donor and acceptor sides of PSII and the

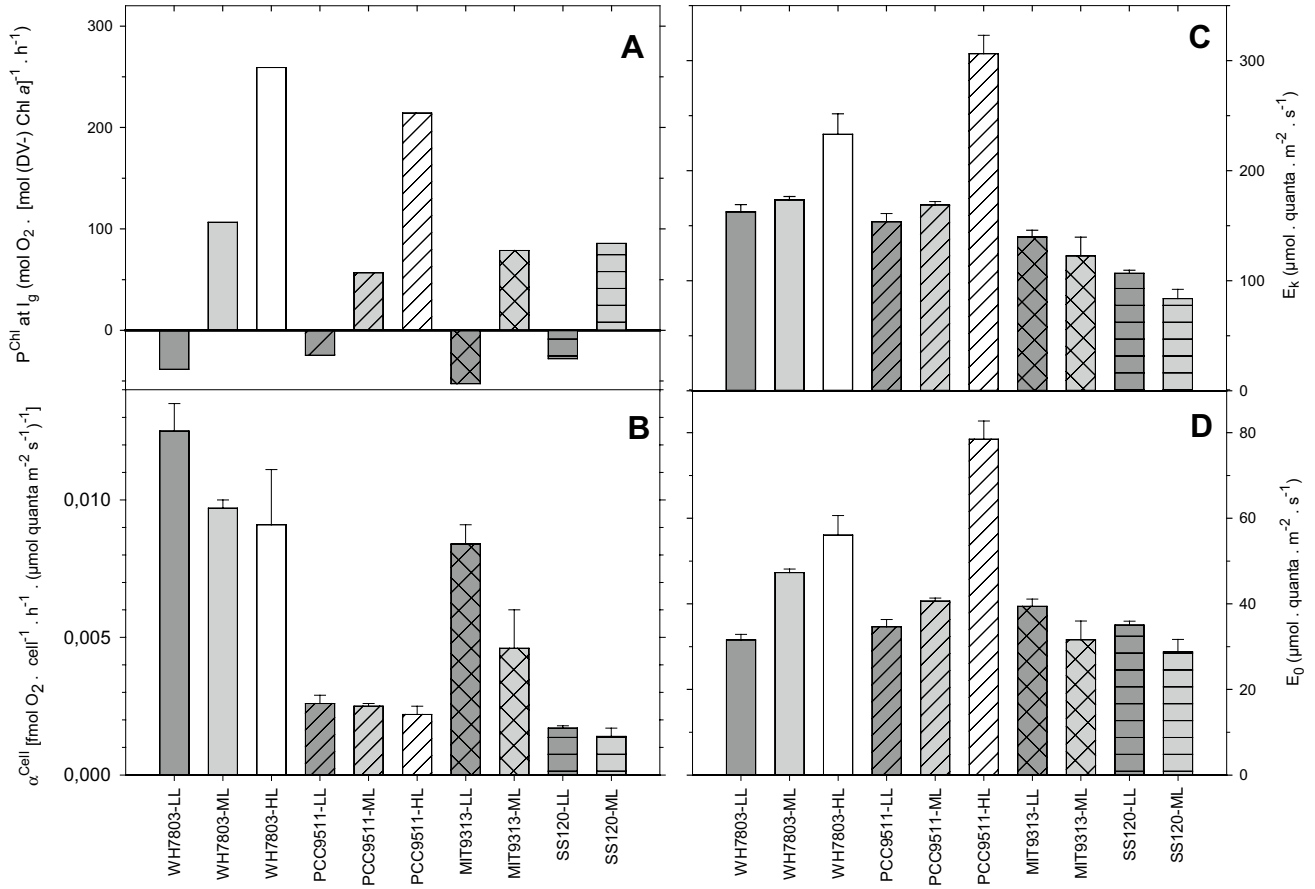

Fig. 2 Photosynthetic parameters derived from the light response curves of oxygen evolution for the four marine picocyanobacterial strains grown at low, medium or high continuous growth irradiance. **a** Oxygen-evolving rates normalized per total Chl at growth irradiance (P^{Chl} at I_g). **b** Photosynthetic capture efficiencies (α) per cell. **c** Saturating irradiance (E_k). **d** Compensation irradiance (E_0)

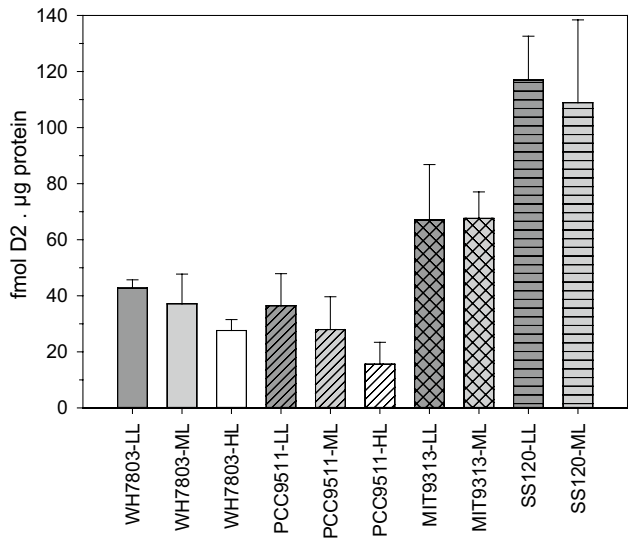

Fig. 3 Molar immunoquantitation of the D2 protein of photosystem II in the four marine picocyanobacterial strains grown at low, medium or high continuous growth irradiance. All measurements are average ± SD of 4 to 6 biological replicates

function of OEC in the studied strains. In the control strain *Synechococcus* sp. WH7803, the glow curve after 2 flashes (the so-called B-band) peaked at 30 °C (Fig. 4a). According to previous results on *Synechocystis* deletion mutants (Burnap et al. 1992; Shen et al. 1997, 1998), one could have expected that the absence of the PsbU or PsbV proteins in the *P. marinus* PCC 9511 and SS120 would result in the shift of the peak temperature of the glow curve to higher temperatures. However, the maxima of all three *Prochlorococcus* strains were either comparable to the control strain or even peaked at lower temperatures (Fig. 4a). Like for WH7803, the $S_{2/3}Q_B^-$ charge recombination in *Prochlorococcus* sp. MIT 9313 resulted in a B-band peaking in the 30–34 °C region, indicating that the recombination of charges stored on $S_2Q_B^-$ and $S_3Q_B^-$ occurs from identical energetic levels. The glow curves of *P. marinus* PCC 9511 were always composed of two bands, peaking around 15 and 32 °C, suggesting a heterogenous energetics of the $S_{2/3}Q_B^-$ charge recombination. Heterogeneity in recombination energetics was also observed in *P. marinus* SS120 (Fig. 4a) and in *Synechocystis* sp. PCC 6803 (data not shown). By adding

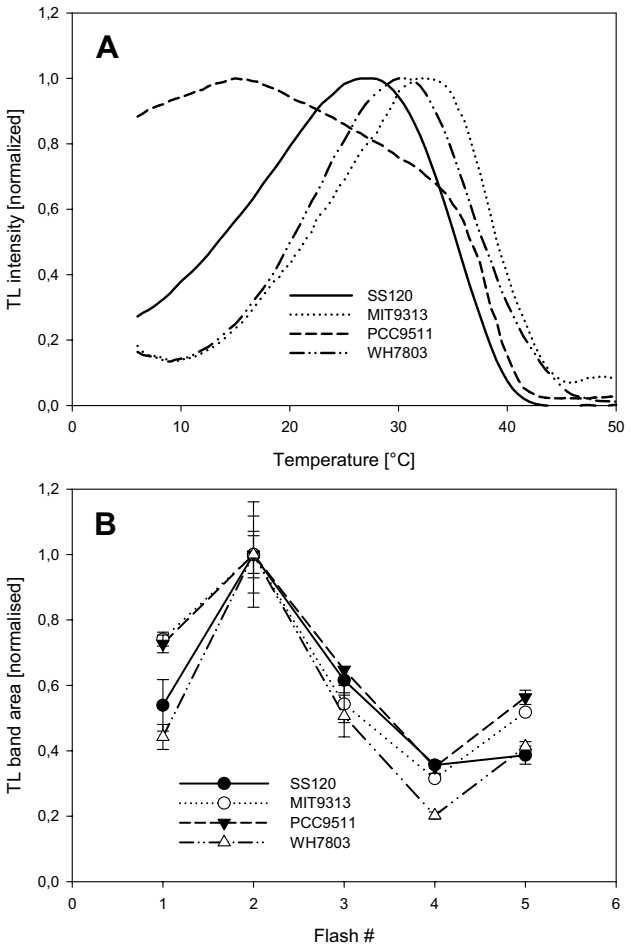

Fig. 4 Thermoluminescence parameters for the picocyanobacteria grown at LL. **a** Plot of normalized thermoluminescence (TL) intensity vs. temperature for the four marine picocyanobacterial strains studied: *Synechococcus* sp. WH7803 and *Prochlorococcus* strains MED4, SS120 and MIT9313. **b** Dependence of the intensity of the B-band on the number of excitation flashes. The intensity of the B-band was calculated as the integral of the TL signal from 10 to 50 °C and normalized to the maximal value reached after 2 flashes

DCMU, we checked that the band at lower temperature was not the Q-band ($S_2Q_A^-$ recombination). The TL glow curve in the presence of DCMU peaked at lower temperatures (-5 to + 5 °C; data not shown). Such heterogeneity likely reflects different energetics of the $S_2Q_B^-$ (B2 band) and $S_3Q_B^-$ (B1 band) charge recombinations in studied organisms. The split in the B-band is typically observed when lumen pH < 7 (Ducruet and Vass 2009). However, in our experiments, the addition of an uncoupler (up to 10 mM NH_4Cl) did not change the shape of the composed B-band (data not shown). We also studied the oscillations of the B-band. Since the TL B-bands result from the $S_{2/3}Q_B^-$ charge recombination only, the overall intensity of the glow curve following excitation by series of single turnover flashes oscillates with period of 4 (Rutherford et al. 1984). Similarly to the oscillations of the oxygen flash yields, these flash-induced oscillations of the TL B-band intensity stem from the initial distribution of the S-states and occupancy of the Q_B pocket in the dark and from the efficiency of transitions between different S-states. Usually, the intensity of the B-band is maximal after two flashes (Rutherford et al. 1984). As expected, in all studied strains, the TL was maximal after two excitation flashes and minimal after 4 flashes (Fig. 4b). One can also note that the B-band was significantly more intense after 1 and 5 excitation flashes in *P. marinus* PCC 9511 and MIT9313, respectively, than in the control *Synechococcus* sp. WH7803 strain (Fig. 4b) or the freshwater *Synechocystis* sp. PCC 6803 (data not shown), where the TL B-band intensity after 1 flash was always less than 45% of the maximum. This increased intensity of the TL glow curve after 1 flash can be interpreted as an increased proportion of PSII centres remaining in the S1 state in the dark in *Prochlorococcus* strains.

We also compared the integral intensity of the TL B-band after 2 pre-flashes normalized to the (DV-)Chl content (Online resource Fig. S6), the TL B-band intensity being a quantitative proxy for the actively recombining PSII reaction centres (Burnap et al. 1992). Similar to the (DV-) Chl-normalized maximal oxygen evolution rates (P^{Chl}_m) at LL (Fig. 1a), the highest Chl-normalized TL emission was detected in *Synechococcus sp*. WH7803, followed by *P. marinus* PCC 9511 and *P. marinus* SS120. However, for unclear reasons, the PSII recombination efficiency was unexpectedly low in *P. marinus* MIT9313, almost an order of magnitude lower than the control WH7803 (0.41 ± 0.12 a.u. and 3.56 ± 0.31 a.u., respectively).

Structural homology model of *P. marinus* MED4 PSII

The published 3D X-ray structure of *Thermosynechococcus elongatus* PSII (Guskov et al. 2009) was used to build a homology model for the PSII of *P. marinus* MED4, a close relative to *P. marinus* PCC 9511 (Rippka et al. 2000). Online Resource_Table_S2 compares the PSII gene content of the four picocyanobacterial strains used in this study and lists all genes included in the model. Comparison of a side view of this MED4 PSII structure (Fig. 5a, c) with the same model where PsbU and PsbV from *T. elongatus* are superimposed (Fig. 5b, d) shows that the Mn cluster of MED4 is directly exposed to the surrounding environment and no structural modifications of PSII proteins surrounding the Mn cluster seemingly compensate for the lack of PsbU and PsbV proteins. This is confirmed by sequence alignments of *T. elongatus* PSII subunits and their orthologs from *Prochlorococcus* and marine *Synechococcus* that show that, despite some intergenus variability in sequences of several minor subunits, most PSII proteins of *Prochlorococcus* strains with

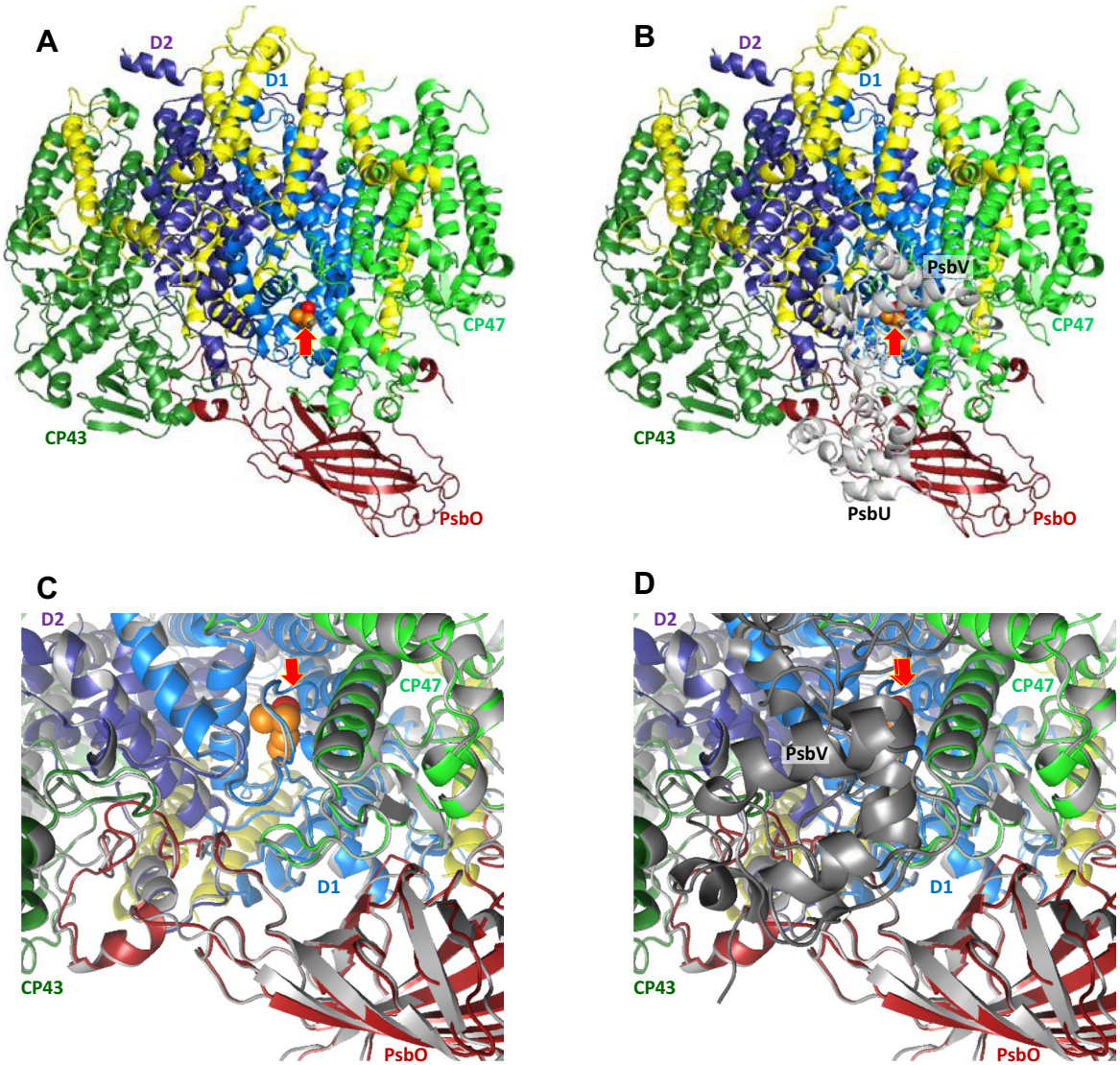

Fig. 5 **a** Luminal side view of the 3D structure of a PSII monomer from *Prochlorococcus marinus* MED4, modelled after *Thermosynechococcus elongatus* (Guskov et al. 2009). **b** Same but showing the location of the PsbU and PsbV proteins from *T. elongatus* that shield the Mn cluster. **c** Zoom on the oxygen-evolving complex (OEC) region with superimposition of the 3D structures of *P. marinus* MED4 (in colour) and *T. elongatus* (in grey). **d** Same as *C* but including the PsbV protein from *T. elongatus* (PsbU cannot be seen on this view). Only the major PSII proteins are annotated; all other intrinsic proteins are shown in yellow (see complete list in Online Resource_Table_S2). The Mn cluster is represented by orange (Mn ions) and red (Ca^{2+} ion) spheres and its position indicated by a red arrow

streamlined genomes are of similar length than their counterparts in marine picocyanobacterial strains possessing PsbU/V (i.e. all *Synechococcus* spp. and/or *Prochlorococcus* sp. clade LLIV; data not shown). Notable exceptions are PsbM and PsbX, two minor PSII proteins that possess a specific extension (C- or N-terminal, respectively) in all streamlined strains (Online Resource_Figs._S7-S8). Yet, the localization of these two proteins on the cytoplasmic side of the PSII structure (Guskov et al. 2009) is way too far from the Mn cluster for these additional domains to compensate for the lack of PsbU and PsbV.

Discussion

Lack of two extrinsic OEC proteins does not affect *P. marinus* oxygen evolution rates

P–E curves and derived parameters showed that *P. marinus* strains PCC 9511 and SS120 can evolve oxygen at significant rates despite lacking *psbU* and *psbV* (Figs. 1, 2 and Online Resource_Fig_S3–S5), even though these two genes appear to be functional in the clade LLIV strain *Prochlorococcus* sp. MIT9313 (Table 1). This contrasts with previous studies on knockout mutants of these genes in freshwater

cyanobacteria, notably regarding the drop of oxygen evolution rates observed in *Synechocystis* sp. PCC 6803 *psbV*-less mutants (Shen et al. 1995, 1998). Yet, examination of a structural homology model of the 3D structure of PSII in *P. marinus* MED4 did not reveal any obvious extension of other PSII subunits located in the close vicinity of the Mn cluster that may compensate for the absence of these extrinsic proteins (Fig. 5a, c). In the PSII structure of *Thermosynechococcus vulcanus*, the PsbV C-terminus, and more specifically Tyr 137, is thought to be involved in an exit channel for protons arising from the deprotonation of D1-Tyr161 (a.k.a. Y_Z) to the lumen (Umena et al. 2011), suggesting that absence of PsbV in MED4 could affect the proton extrusion process. It is worth noting that PsbU and PsbV are also absent from green algae and higher plants, but they are replaced by PsbP and PsbQ (De Las Rivas et al. 2007). Surprisingly, most cyanobacteria possess distant PsbP and PsbQ homologs, usually called 'CyanoP' and 'CyanoQ', respectively (Kashino et al. 2002; Thornton et al. 2004; Roose et al. 2007; Enami et al. 2008), but their role and localization remain unclear, since they are not detected in PSII crystal structures (Guskov et al. 2009; Umena et al. 2011). While the *cyanoQ* gene is absent from all *Prochlorococcus* genomes, including members of the LLIV clade, *cyanoP* is a core gene in marine picocyanobacteria (Online Resource_Table_S2). CyanoP is thought to be a constitutive PSII protein that stabilizes charge separation (Sato 2010; Aoi et al. 2014). As previously noticed by Fagerlund and Eaton-Rye (2011), its closest homolog in *Arabidopsis* is not PsbP itself, but the PsbP-like protein encoded by *PPL1* (*At3g55330*), which is involved in the repair of photodamaged PSII (Ishihara et al. 2007). *In silico* protein docking experiments have suggested that, when CyanoQ is present, CyanoP is located on the lumenal face of the PSII complex, below the D2 protein and away from the other extrinsic proteins. However, in absence of CyanoQ, CyanoP might take its place in the immediate vicinity of PsbV (Fagerlund and Eaton-Rye 2011). So, we cannot exclude that in *P. marinus* MED4, which lacks PsbU, PsbV and CyanoQ altogether, CyanoP might have a role in shielding the Mn cluster. Another noticeable PSII protein present in all marine picocyanobacteria (Online Resource_Table_S2), but not in PSII crystals, is Psb27 (Nowaczyk et al. 2006). Like CyanoP (and CyanoQ), it possesses an N-terminal signal peptidase II motif, indicating that it is a lipoprotein. In *Synechocystis* PCC 6803, Psb27 is thought to facilitate the assembly of the Mn cluster by preventing the premature association of other extrinsic proteins (PsbO, PsbU, PsbV and CyanoQ). Psb27 is then replaced by these proteins upon assembly of the Mn cluster (Roose and Pakrasi 2008). Psb27 has been reported to occur in sub-stoichiometric amounts compared to other PSII subunits in *T. elongatus* (Michoux et al. 2014). If this is also the case in *Prochlorococcus* strains lacking PsbU and PsbV, this would plead against a role of Psb27 in shielding of the Mn cluster. However, one cannot exclude that the absence of *psbU* and *psbV* in many *Prochlorococcus* strains might trigger an increased expression level for *psb27*, so that its product would be synthesized in stoichiometric amounts compared to other PSII components and could act as a constitutive OEC extrinsic protein. Examination of the whole transcriptome of *P. marinus* MED4 cells synchronized by a 14-h:10-h light–dark cycle (Zinser et al. 2009) indeed shows that *psb27* is strongly expressed and exhibits a diel cycle globally similar to *psbO*, with a maximum at the dark-to-light transition and a minimum in the afternoon, while *cyanoP* and *psb27* both reach their minimal diel expression level 2 h before *psbO* (4 pm *vs*. 6 pm, respectively; see http://proportal.mit.edu/).

Another possibility is that the missing PsbU and PsbV have been replaced by some *Prochlorococcus*-specific PSII protein(s) that could have been acquired early during the evolution of these lineages. The comparison of currently available genomes of marine picocyanobacteria shows that *Prochlorococcus* strains with a streamlined genome possess 21 specific proteins (absent from both *Prochlorococcus* spp. LLIV and *Synechococcus* spp. strains; Online Resource Table S3). However, examination of these sequences using LipoP (http://www.cbs.dtu.dk/services/LipoP/) shows that none contain a putative N-terminal signal peptidase II motif, indicative of lipoproteins (as found in CyanoP and CyanoQ), nor even a signal peptidase I motif (as found in PsbU and PsbV). A number of uncharacterized membrane proteins are, however, worth noting in this dataset, as they could potentially intrinsic PSII proteins specific of *Prochlorococcus* with streamlined genomes (Online Resource Table S3).

Proteins able to replace PsbU and/or PsbV might also have been acquired later during the evolution of the *Prochlorococcus* radiation, i.e. by the common ancestor of the HL branch shortly after its differentiation from other (LL-adapted) *Prochlorococcus* lineages. The rationale for this hypothesis is that a *psbU*-less mutant of *Synechocystis* sp. PCC 6803 was found to grow well under moderate light, but was highly susceptible to photoinhibition at high light, likely due to an accelerated rate of D1 degradation in this condition (Inoue-Kashino et al. 2005). The absence of the Mn cluster shield provided by PsbU might therefore not be harmful for *Prochlorococcus* cells living in a low light habitat like that occupied by LL-adapted *P. marinus* (such as SS120), while it would be deleterious in the upper mixed layer that is exposed to high irradiances, where thrive HL-adapted strains *P. marinus*, such as MED4 or PCC 9511. Comparative genomics analyses showed that sequenced members of the HL clades possess at least 76 specific genes (i.e. absent from all other marine picocyanobacteria), including one (PMM0736) for which LipoP detected a signal peptidase II motif (like in CyanoP and

CyanoQ) and nine others that exhibited (like for PsbU/V) a signal peptidase I motif (Online Resource Table S3). Proteomic analyses of PSII preparations are needed to check whether some of the abovementioned proteins are indeed linked to PSII and/or localized near the OEC.

Alternatively, compensatory mechanisms for the lack of extrinsic proteins in *Prochlorococcus* cells may simply rely on the occurrence in *Prochlorococcus* cells of an ion environment in the thylakoid lumen that could be different from that in freshwater cyanobacteria, especially regarding Ca^{2+} and Cl^{-}, a difference possibly linked to their different habitat. Indeed, both of these OEC cofactors were shown to be critical for the growth of a *Synechocystis* sp. PCC 6803 *psbU*- and psb*V*-less mutant, likely due to their protective role on the Mn cluster, by reducing its accessibility to solvent attacks (Shen et al. 1998; Inoue-Kashino et al. 2005).

Insights from the thermoluminescence analysis

TL has been used as a tool to study the role of extrinsic OEC proteins in model cyanobacteria (Balint et al. 2006; Burnap et al. 1992; Shen et al. 1997, 1998). The deletion of PsbU and PsbV was found to cause a shift of the B-band to higher temperatures and a lower intensity of the B-band, suggesting a stabilization of the S_2 state of the OEC and a decrease in the number of active PSII centres. Although each *Prochlorococcus* strain that we studied had distinct and characteristic shape of the B-band (Online Resource_Fig_S6), we did not observe any clear trend in B-band shape or peak position that could be explained by the absence of the extrinsic proteins, indicating that the OEC is fully functional in strains with streamlined genomes. When studying the oscillation patterns of the TL B-band (Fig. 4b), we noticed that, in all *Prochlorococcus* strains, the TL intensity after one flash was significantly higher than in all other cyanobacteria or microalgae studied in recent years in the Třeboň laboratory (data not shown). Since we still observed maxima after 2 flashes, we interpret this modification of the TL oscillation pattern not as a change of the Q_B/Q_B^- fraction but rather as an increase in the fraction of centres in S_1 state in the dark. TL intensity can be used also as a proxy for active PSII centres (Burnap et al. 1992). Such proxy is, however, only semi-quantitative because several pathways for the $S_{2/3}Q_B^-$ charge recombination exist within PSII and TL monitors only one of them, namely the radiative recombination resulting in the singlet P_{680}*. Still, we observed reasonable correlation between the P^{Chl}_m and the (DV-)Chl-normalized TL intensity for three of the studied strains grown at LL (Online Resource Fig S6, inset). Yet, the reason for the much lower TL intensity observed in the MIT9313 strain remains unclear and would require further experimental work.

Comparison of *Prochlorococcus* oxygen evolution and carbon assimilation rates

While several previous studies reported carbon fixation rates in various *Prochlorococcus* strains (Bruyant et al. 2005; Partensky et al. 1993; Moore and Chisholm 1999; Zinser et al. 2009) and in *Synechococcus* sp. WH7803 (Kana and Glibert 1987b), the present study is to our knowledge the first one reporting in detail oxygen production in marine picocyanobacteria. A striking feature of P–E curves derived from incubations with $^{14}CO_2$ of both LL- and HL-adapted *Prochlorococcus* strains (but not *Synechococcus*) is the strong photoinhibitory effect of high irradiances, as indicated by a drop in P^{Chl} at irradiances ca. fourfold higher than the light saturation index E_k (Partensky et al. 1993; Moore and Chisholm 1999). In contrast, we observed little photoinhibition in the present study, even for the LL-adapted strains (Online Resource_Fig_S3–S5), though it is worth noting that MIT9313 cultures pre-acclimated to 75 ± 10 µmol quanta m^{-2} s^{-1} did show an altered O_2 emission after 4–5 min exposure to the highest tested irradiance; see Online Resource_Fig_S1. This difference is possibly due to the fact that the method used to measure O_2 evolution, typically 5–10 min exposure to light followed by a similar period in dark (Online Resource_Fig_S1), is much less stressing for *Prochlorococcus* cells than are measurements of CO_2 assimilation. For instance, for modelling P–E curves Moore and Chisholm (1999) exposed cells to a range of irradiances for 45 min.

The photosynthetic quotient, i.e. the number of moles O_2 produced per mole CO_2 assimilated, has not yet been determined for *Prochlorococcus*. However, since all *Prochlorococcus* strains studied here lack nitrate assimilation genes and cells essentially rely on ammonium as a nitrogen source (Kettler et al. 2007; Rocap et al. 2003; Moore et al. 2002), therefore avoiding the electron-consuming step of nitrate reduction, the photosynthetic quotient should theoretically not deviate much from 1.0 (Falkowski and Raven 2007). This makes possible direct comparisons between maximum photosynthetic rates for O_2 production and CO_2 consumption. Moore and Chisholm (1999) measured P^{Chl}_m values of ca. 134, 156 and 179 mol C mol Chl a^{-1} h^{-1} at LL, as compared in the present study to 226, 173 and 342 mol O_2 mol Chl a^{-1} h^{-1} at LL for PCC 9511 (a close relative of MED4), SS120 and MIT9313, respectively. Although P^{Chl}_m values obtained here for O_2 release were systematically higher than Moore and co-workers' for CO_2 assimilation, these discrepancies might be due in part to the different light conditions used in the two studies.

Ecological implications of *Prochlorococcus* oxygen evolution characteristics

The O_2 evolving measurements reported in the present study for different strains of marine picocyanobacteria at several growth irradiances should be very useful for assessing the contribution of these key phytoplankters to the global oxygen production of the world ocean and more generally their role in the biogeochemical cycle of oxygen. Our study also provides new insights to explain the paradoxical occurrence of virtually monoalgal populations of *Prochlorococcus* in waters of the Arabian Sea and the Eastern Tropical Pacific Ocean displaying O_2 concentrations lower than 20 µM, so-called 'oxygen minimum zones' (OMZ; Beman and Carolan 2013; Garcia-Robledo et al. 2017; Goericke et al. 2000; Lavin et al. 2010). OMZ generally occur along continental margins where high rates of phytoplankton productivity in the upper layer, coupled with poor ventilation and sluggish circulation, lead to an extensive, oxygen-deficient layer at depth, where the decomposition of sinking biological material provokes high microbial respiration rates (Helly and Levin 2004). Although most of the OMZ occur below the euphotic layer, the top of the OMZ can be reached by light and when this is the case, O_2 production by *Prochlorococcus* could be sufficient to feed aerobic processes (Ulloa et al. 2012). The maintenance of anoxic conditions despite vertical mixing and lateral advection was proposed to rely upon highly efficient O_2 scavenging by local microbial communities (Kalvelage et al. 2015). However, our data show that at the low irradiances reaching the top of the OMZ (typically 0.1 to 2% of the surface irradiance; (Goericke et al. 2000; Garcia-Robledo et al. 2017), corresponding to ca. 2–40 µmol quanta m^{-2} s^{-1} at solar noon), the net oxygen exchange rate of *Prochlorococcus* cells is expected to be less than or equal to zero (Online Resource_Fig_S3A). This could explain in part the very low oxygen levels measured in these layers. Phylogenetic analyses of *Prochlorococcus* populations thriving in OMZ showed that they predominantly belong to the LLIV clade and to two novel, uncultured low light-adapted clades called LLV and LLVI (Lavin et al. 2010). The latter clades are phylogenetically closely related to LLIV members and share a number of characteristics with them, such as a large G+C% compared to other *Prochlorococcus* lineages. It is therefore possible that, like MIT9313, their genome is not streamlined and that they possess a full set of OEC proteins, a hypothesis that will be confirmed by sequencing the genomes of LLV and LLVI representatives.

Acknowledgements This work was funded by the collaborative program between CNRS and the Czech Academy of Sciences (PICS Oxybac). O.P. and E.K. are currently funded by the project "Algatech plus" (Czech Ministry of Education, programme NPU 1, #LO 1416). We are grateful members of the Roscoff Culture Collection for providing *Prochlorococcus* and *Synechococcus* strains used in this study.

References

Aoi M, Kashino Y, Ifuku K (2014) Function and association of CyanoP in photosystem II of *Synechocystis* sp. PCC 6803. Res Chem Intermediat 40:3209–3217. https://doi.org/10.1007/s11164-014-1827-y

Balint I, Bhattacharya J, Perelman A, Schatz D, Moskovitz Y, Keren N, Schwarz R (2006) Inactivation of the extrinsic subunit of photosystem II, PsbU, in *Synechococcus* PCC 7942 results in elevated resistance to oxidative stress. FEBS Lett 580:2117–2122. https://doi.org/10.1016/j.febslet.2006.03.020

Batut B, Knibbe C, Marais G, Daubin V (2014) Reductive genome evolution at both ends of the bacterial population size spectrum. Nature Rev Microbiol 12:841–850. https://doi.org/10.1038/nrmicro3331

Belgio E, Trsková E, Kotabová E, Ewe D, Prášil O, Kana R (2018) High light acclimation of *Chromera velia* points to photoprotective NPQ. Photosynth Res 135:263–274. https://doi.org/10.1007/s11120-017-0385-8

Beman JM, Carolan MT (2013) Deoxygenation alters bacterial diversity and community composition in the ocean's largest oxygen minimum zone. Nature Commun 4:2705. https://doi.org/10.1038/Ncomms3705

Biller SJ, Berube PM, Berta-Thompson JW, Kelly L, Roggensack SE, Awad L, Roache-Johnson KH, Ding H, Giovannoni SJ, Rocap G, Moore LR, Chisholm SW (2014) Genomes of diverse isolates of the marine cyanobacterium *Prochlorococcus*. Nature Scient Data 1:140034. https://doi.org/10.1038/sdata.2014.34

Brand LE, Guillard RRL, Murphy LS (1981) A method for the rapid and precise determination of acclimated phytoplankton reproduction rates. J Plankt Res 3:193–201. https://doi.org/10.1093/plankt/3.2.193

Bruyant F, Babin M, Genty B, Prasil O, Behrenfeld MJ, Claustre H, Bricaud A, Garczarek L, Holtzendorff J, Koblizek M, Dousova H, Partensky F (2005) Diel variations in the photosynthetic parameters of *Prochlorococcus* strain PCC 9511: Combined effects of light and cell cycle. Limnol Oceanogr 50:850–863. https://doi.org/10.4319/lo.2005.50.3.0850

Burnap RL, Shen JR, Jursinic PA, Inoue Y, Sherman LA (1992) Oxygen yield and thermoluminescence characteristics of a cyanobacterium lacking the manganese-stabilizing protein of photosystem II. Biochemistry 31:7404–7410. https://doi.org/10.1021/bi00147a027

Campbell L, Vaulot D (1993) Photosynthetic picoplankton community structure in the subtropical North Pacific Ocean near Hawaii (station ALOHA). Deep Sea Res 40:2043–2060. https://doi.org/10.1016/0967-0637(93)90044-4

Campbell L, Nolla HA, Vaulot D (1994) The importance of *Prochlorococcus* to community structure in the central North Pacific Ocean. Limnol Oceanogr 39:954–961. https://doi.org/10.4319/lo.1994.39.4.0954

Chen M, Zhang Y, Blankenship RE (2008) Nomenclature for membrane-bound light-harvesting complexes of cyanobacteria. Photosynth Res 95:147–154. https://doi.org/10.1016/j.bbabio.2013.07.012

De Las Rivas J, Balsera M, Barber J (2004) Evolution of oxygenic photosynthesis: Genome-wide analysis of the OEC extrinsic proteins. Trends Plant Sci 9:18–25. https://doi.org/10.1016/j.tplants.2003.11.007

De Las Rivas J, Heredia P, Roman A (2007) Oxygen-evolving extrinsic proteins (PsbO,P,Q,R): Bioinformatic and functional analysis. Biochim Biophys Acta 1767:575–582. https://doi.org/10.1016/j.bbabio.2007.01.018

DeLano WL (2002) The PyMOL Molecular Graphics System San Carlos. CA, USA

Ducruet JM, Vass I (2009) Thermoluminescence: experimental. Photosynth Res 101:195–204. https://doi.org/10.1007/s11120-009-9436-0

Dufresne A, Garczarek L, Partensky F (2005) Accelerated evolution associated with genome reduction in a free-living prokaryote. Genome Biol 6:R14. https://doi.org/10.1186/gb-2005-6-2-r14

Dufresne A, Ostrowski M, Scanlan DJ, Garczarek L, Mazard S, Palenik BP, Paulsen IT, Tandeau de Marsac N, Wincker P, Dossat C, Ferriera S, Johnson J, Post AF, Hess WR, Partensky F (2008) Unraveling the genomic mosaic of a ubiquitous genus of marine cyanobacteria. Genome Biol 9:R90. https://doi.org/10.1186/gb-2008-9-5-r90

Enami I, Yoshihara S, Tohri A, Okumura A, Ohta H, Shen JR (2000) Cross-reconstitution of various extrinsic proteins and photosystem II complexes from cyanobacteria, red alga and higher plant. Plant Cell Physiol 41:1354–1364. https://doi.org/10.1007/s11120-004-7760-y

Enami I, Okumura A, Nagao R, Suzuki T, Iwai M, Shen JR (2008) Structures and functions of the extrinsic proteins of photosystem II from different species. Photosynth res 98:349–363. https://doi.org/10.1007/s11120-008-9343-9

Eswar N, Webb B, Marti-Renom MA, Madhusudhan MS, Eramian D, Shen M-Y, Pieper U, Sali A (2007) Comparative protein structure modeling using MODELLER. Curr Protoc Protein Sci. https://doi.org/10.1002/0471140864.ps0209s50

Fagerlund RD, Eaton-Rye JJ (2011) The lipoproteins of cyanobacterial photosystem II. J Photoch Photobiol 104:191–203. https://doi.org/10.1016/j.jphotobiol.2011.01.022

Falkowski P, Raven J (2007) Aquatic photosynthesis. 2nd edn. Princeton University Press, Princeton

Ferreira KN, Iverson TM, Maghlaoui K, Barber J, Iwata S (2004) Architecture of the photosynthetic oxygen-evolving center. Science 303:1831–1838. https://doi.org/10.1126/science.1093087

Flombaum P, Gallegos JL, Gordillo RA, Rincon J, Zabala LL, Jiao N, Karl DM, Li WK, Lomas MW, Veneziano D, Vera CS, Vrugt JA, Martiny AC (2013) Present and future global distributions of the marine Cyanobacteria *Prochlorococcus* and *Synechococcus*. Proc Natl Acad Sci USA 110:9824–9829. https://doi.org/10.1073/pnas.1307701110

Garcia-Robledo E, Padilla CC, Aldunate M, Stewart FJ, Ulloa O, Paulmier A, Gregori G, Revsbech NP (2017) Cryptic oxygen cycling in anoxic marine zones. Proc Natl Acad Sci USA 114:8319–8324

Garczarek L, Dufresne A, Blot N, Cockshutt AM, Peyrat A, Campbell DA, Joubin L, Six C (2008) Function and evolution of the *psbA* gene family in marine *Synechococcus: Synechococcus* sp. WH7803 as a case study. ISME J 2:937–953. https://doi.org/10.1038/ismej.2008.46

Geider RJ, Osborne BA (1992) The photosynthesis-light response curve. In: Geider RJ, Osborne BA (eds) Algal Photosynthesis: the measurement of algal gas exchange. Current phycology. Springer, Dordrecht, pp 156–191. https://doi.org/10.1007/978-1-4757-2153-9_7

Glibert PM, Kana TM, Olson RJ, Kirchman DL, Alberte RS (1986) Clonal comparisons of growth and photosynthetic responses to nitrogen availability in marine *Synechococcus* spp. J Exp Mar Biol Ecol 101:199–208. https://doi.org/10.1016/0022-0981(86)90050-X

Goericke R, Repeta DJ (1992) The pigments of *Prochlorococcus marinus*: the presence of divinyl chlorophyll *a* and *b* in a marine prochlorophyte. Limnol Oceanogr 37:425–433. https://doi.org/10.4319/lo.1992.37.2.0425

Goericke R, Olson RJ, Shalapyonok A (2000) A novel niche for *Prochlorococcus* sp in low-light suboxic environments in the Arabian Sea and the Eastern Tropical North Pacific. Deep Sea Res Pt I 47:1183–1205. https://doi.org/10.1016/S0967-0637(99)00108-9

Guskov A, Kern J, Gabdulkhakov A, Broser M, Zouni A, Saenger W (2009) Cyanobacterial photosystem II at 2.9-angstrom resolution and the role of quinones, lipids, channels and chloride. Nat Struct Mol Biol 16:334–342. https://doi.org/10.1038/nsmb.1559

Helly JJ, Levin LA (2004) Global distribution of naturally occurring marine hypoxia on continental margins. Deep Sea Res Pt I 51:1159–1168. https://doi.org/10.1016/j.dsr.2004.03.009

Hess WR, Partensky F, Van der Staay GWM, Garcia-Fernandez JM, Boerner T, Vaulot D (1996) Coexistence of phycoerythrin and a chlorophyll *a/b* antenna in a marine prokaryote. Proc Natl Acad Sci USA 93:11126–11130

Inoue-Kashino N, Kashino Y, Satoh K, Terashima I, Pakrasi HB (2005) PsbU provides a stable architecture for the oxygen-evolving system in cyanobacterial photosystem II. Biochemistry 44:12214–12228. https://doi.org/10.1021/bi047539k

Ishihara S, Takabayashi A, Ido K, Endo T, Ifuku K, Sato F (2007) Distinct functions for the two PsbP-like proteins PPL1 and PPL2 in the chloroplast thylakoid lumen of *Arabidopsis*. Plant Physiol 145:668–679. https://doi.org/10.1104/pp.107.105866

Kalvelage T, Lavik G, Jensen MM, Revsbech NP, Loscher C, Schunck H, Desai DK, Hauss H, Kiko R, Holtappels M, LaRoche J, Schmitz RA, Graco MI, Kuypers MMM (2015) Aerobic microbial respiration in oceanic oxygen minimum zones. PloS ONE 10:e0133526. https://doi.org/10.1371/journal.pone.0133526

Kana TM, Glibert PM (1987a) Effect of irradiances up to 2000 μE m^{-2} s^{-1} on marine *Synechococcus* WH7803 - I. Growth, pigmentation, and cell composition. Deep Sea Res 34:479–485. https://doi.org/10.1016/0198-0149(87)90001-X

Kana TM, Glibert PM (1987b) Effect of irradiances up to 2000 μE m^{-2} s^{-1} on marine *Synechococcus* WH7803 - II. Photosynthetic responses mechanisms. Deep Sea Res 34:497–516. https://doi.org/10.1016/0198-0149(87)90002-1

Kashino Y, Lauber WM, Carroll JA, Wang Q, Whitmarsh J, Satoh K, Pakrasi HB (2002) Proteomic analysis of a highly active photosystem II preparation from the cyanobacterium *Synechocystis* sp. PCC 6803 reveals the presence of novel polypeptides. Biochemistry 41:8004–8012. https://doi.org/10.1021/bi026012&%23x002B;

Kawakami K, Umena Y, Kamiya N, Shen JR (2011) Structure of the catalytic, inorganic core of oxygen-evolving photosystem II at 1.9 angstrom resolution. J Photochem Photobiol 104:9–18. https://doi.org/10.1016/j.jphotobiol.2011.03.017

Kettler G, Martiny AC, Huang K, Zucker J, Coleman ML, Rodrigue S, Chen F, Lapidus A, Ferriera S, Johnson J, Steglich C, Church G, Richardson P, Chisholm SW (2007) Patterns and implications of gene gain and loss in the evolution of *Prochlorococcus*. PLoS Genet 3:e231. https://doi.org/10.1371/journal.pgen.0030231

Kimura A, Eaton-Rye JJ, Morita EH, Nishiyama Y, Hayashi H (2002) Protection of the oxygen-evolving machinery by the extrinsic proteins of photosystem II is essential for development of cellular thermotolerance in *Synechocystis* sp PCC 6803. Plant Cell Physiol 43:932–938. https://doi.org/10.1093/pcp/pcf110

Lavin P, Gonzalez B, Santibanez JF, Scanlan DJ, Ulloa O (2010) Novel lineages of *Prochlorococcus* thrive within the oxygen minimum zone of the eastern tropical South Pacific. Environ Microbiol Rep 2:728–738. https://doi.org/10.1111/j.1758-2229.2010.00167.x

Li WKW (1994) Primary productivity of prochlorophytes, cyanobacteria, and eucaryotic ultraphytoplankton: measurements from flow cytometric sorting. Limnol Oceanogr 39:169–175. https://doi.org/10.4319/lo.1994.39.1.0169

Li WKW, Dickie PM, Irwin BD, Wood AM (1992) Biomass of bacteria, cyanobacteria, prochlorophytes and photosynthetic eukaryotes in the Sargasso Sea. Deep Sea Res 39:501–519. https://doi.org/10.1016/0198-0149(92)90085-8

Liu HB, Nolla HA, Campbell L (1997) *Prochlorococcus* growth rate and contribution to primary production in the equatorial and subtropical North Pacific Ocean. Aquat Microb Ecol 12:39–47

Marie D, Partensky F, Vaulot D, Brussaard C (1999) Enumeration of phytoplankton, bacteria, and viruses in marine samples. Current Protocol Cytom 10:11. https://doi.org/10.1002/0471142956.cy1111s10 11.11–11.11.15.

Michoux F, Boehm M, Bialek W, Takasaka K, Maghlaoui K, Barber J, Murray JW, Nixon PJ (2014) Crystal structure of CyanoQ from the thermophilic cyanobacterium *Thermosynechococcus elongatus* and detection in isolated photosystem II complexes. Photosynth Res 122:57–67. https://doi.org/10.1007/s11120-014-0010-z

Moore LR, Chisholm SW (1999) Photophysiology of the marine cyanobacterium *Prochlorococcus*: Ecotypic differences among cultured isolates. Limnol Oceanogr 44:628–638. https://doi.org/10.4319/lo.1999.44.3.0628

Moore LR, Post AF, Rocap G, Chisholm SW (2002) Utilization of different nitrogen sources by the marine cyanobacteria *Prochlorococcus* and *Synechococcus*. Limnol Oceanogr 47:989–996. https://doi.org/10.4319/lo.2002.47.4.0989

Nishiyama Y, Los DA, Hayashi H, Murata N (1997) Thermal protection of the oxygen-evolving machinery by PsbU, an extrinsic protein of photosystem II, in *Synechococcus* species PCC 7002. Plant Physiol 115:1473–1480. https://doi.org/10.1104/pp.115.4.1473

Nishiyama Y, Los DA, Murata N (1999) PsbU, a protein associated with photosystem II, is required for the acquisition of cellular thermotolerance in *Synechococcus* species PCC 7002. Plant Physiol 120:301–308. https://doi.org/10.1104/pp.120.1.301

Nowaczyk MM, Hebeler R, Schlodder E, Meyer HE, Warscheid B, Rogner M (2006) Psb27, a cyanobacterial lipoprotein, is involved in the repair cycle of photosystem II. Plant Cell 18:3121–3131. https://doi.org/10.1105/tpc.106.042671

Okumura A, Ohta H, Inoue Y, Enami I (2001) Identification of functional domains of the extrinsic 12 kDa protein in red algal PSII by limited proteolysis and directed mutagenesis. Plant Cell Physiol 42:1331–1337

Okumura A, Sano M, Suzuki T, Tanaka H, Nagao R, Nakazato K (2007) Aromatic structure of tyrosine-92 in the extrinsic PsbU protein of red algal photosystem II is important for its functioning. FEBS Lett 581:5255–5258. https://doi.org/10.1016/j.febslet.2007.10.015

Partensky F, Garczarek L (2003) The photosynthetic apparatus of chlorophyll *b*- and *d*-containing Oxychlorobacteria. In: Larkum AWD, Douglas SE, Raven JA (eds) Photosynthesis in Algae. Advances in Photosynthesis Series, vol 14. Kluwer Academic Publishers, Dordrecht, pp 29–62. https://doi.org/10.1007/978-94-007-1038-2_3

Partensky F, Garczarek L (2010) *Prochlorococcus*: Advantages and limits of minimalism. Ann Rev Mar Sci 2:305–331. https://doi.org/10.1146/annurev-marine-120308-081034

Partensky F, Hoepffner N, Li WKW, Ulloa O, Vaulot D (1993) Photoacclimation of *Prochlorococcus* sp. (Prochlorophyta) strains isolated from the North Atlantic and the Mediterranean Sea. Plant Physiol 101(1):285–296. https://doi.org/10.1104/pp.101.1.285

Pittera J, Humily F, Thorel M, Grulois D, Garczarek L, Six C (2014) Connecting thermal physiology and latitudinal niche partitioning in marine *Synechococcus*. ISME J 8:1221–1236. https://doi.org/10.1038/ismej.2013.228

Platt T, Jassby AD (1976) Relationship between photosynthesis and light for natural assemblages of coastal marine-phytoplankton. J Phycol 12:421–430. https://doi.org/10.1111/j.1529-8817.1976.tb02866.x

Porra RJ (2002) The chequered history of the development and use of simultaneous equations for the accurate determination of chlorophylls *a* and *b*. Photosynthesis research 73:149–156. https://doi.org/10.1023/A:1020470224740

Rippka R, Coursin T, Hess W, Lichtlé C, Scanlan DJ, Palinska KA, Iteman I, Partensky F, Houmard J, Herdman M (2000) *Prochlorococcus marinus* Chisholm et al. 1992 *subsp. pastoris subsp. nov*. strain PCC 9511, the first axenic chlorophyll a_2/b_2-containing cyanobacterium (Oxyphotobacteria). Int J Syst Evol Microbiol 50:1833–1847. https://doi.org/10.1099/00207713-50-5-1833

Rocap G, Larimer FW, Lamerdin J, Malfatti S, Chain P, Ahlgren NA, Arellano A, Coleman M, Hauser L, Hess WR, Johnson ZI, Land M, Lindell D, Post AF, Regala W, Shah M, Shaw SL, Steglich C, Sullivan MB, Ting CS, Tolonen A, Webb EA, Zinser ER, Chisholm SW (2003) Genome divergence in two *Prochlorococcus* ecotypes reflects oceanic niche differentiation. Nature 424:1042–1047. https://doi.org/10.1038/nature01947

Roose JL, Pakrasi HB (2008) The Psb27 protein facilitates manganese cluster assembly in photosystem II. J Biol Chem 283:4044–4050. https://doi.org/10.1074/jbc.M708960200

Roose JL, Kashino Y, Pakrasi HB (2007) The PsbQ protein defines cyanobacterial Photosystem II complexes with highest activity and stability. Proc Natl Acad Sci USA 104:2548–2553. https://doi.org/10.1073/pnas.0609337104

Roussel A, Cambillau C (1991) TURBO-FRODO: a tool for building structural models. In: Directory SGGP (ed) Silicon Graphics. Mountain View, CA, p 86

Roy S, Llewellyn CA, Skarstad Egeland E, Johnsen G (2011) Phytoplankton pigments, characterization, chemotaxonomy and applications in oceanography. Cambridge Environmental Chemistry Series. Cambridge University Press, Cambridge

Rutherford AW, Inoue Y (1984) Charge accumulation and photochemistry in leaves studied by thermoluminescence and delayed light emission. Proc Natl Acad Sci USA 81:1107–1111

Sato N (2010) Phylogenomic and structural modeling analyses of the PsbP superfamily reveal multiple small segment additions in the evolution of photosystem II-associated PsbP protein in green plants. Mol Phylogenet Evol 56:176–186. https://doi.org/10.1016/j.ympev.2009.11.021

Scanlan DJ, Ostrowski M, Mazard S, Dufresne A, Garczarek L, Hess WR, Post AF, Hagemann M, Paulsen I, Partensky F (2009) Ecological genomics of marine picocyanobacteria. Microbiol Mol Biol Rev 73:249–299. https://doi.org/10.1128/MMBR.00035-08

Shen JR, Vermaas W, Inoue Y (1995) The role of cytochrome c-550 as studied through reverse genetics and mutant characterization in *Synechocystis* sp. PCC 6803. J Biol Chem 270:6901–6907. https://doi.org/10.1074/jbc.270.12.6901

Shen JR, Ikeuchi M, Inoue Y (1997) Analysis of the *psbU* gene encoding the 12-kDa extrinsic protein of photosystem II and studies on its role by deletion mutagenesis in *Synechocystis* sp. PCC 6803. J Biol Chem 272:17821–17826. https://doi.org/10.1074/jbc.272.28.17821

Shen JR, Qian M, Inoue Y, Burnap RL (1998) Functional characterization of *Synechocystis* sp. PCC 6803 delta-*psbU* and delta-*psbV* mutants reveals important roles of cytochrome c-550 in cyanobacterial oxygen evolution. Biochemistry 37:1551–1558. https://doi.org/10.1021/bi971676i

Six C, Finkel ZV, Irwin AJ, Campbell DA (2007) Light variability illuminates niche-partitioning among marine picocyanobacteria. PloS One 2:e1341. https://doi.org/10.1371/journal.pone.0001341

Stockner JG (1988) Phototrophic picoplankton: an overview from marine and freshwater ecosystems. Limnol Oceanogr 33:765–775. https://doi.org/10.4319/lo.1988.33.4part2.0765

Thompson JD, Higgins DG, Gibson TJ (1994) Clustal-W - Improving the sensitivity of progressive multiple sequence alignment through sequence weighting, position-specific gap penalties and weight matrix choice. Nucleic Acids Res 22:4673–4680. https://doi.org/10.1007/978-1-4020-6754-9_3188

Thornton LE, Ohkawa H, Roose JL, Kashino Y, Keren N, Pakrasi HB (2004) Homologs of plant PsbP and PsbQ proteins are necessary for regulation of photosystem II activity in the cyanobacterium *Synechocystis* 6803. Plant Cell 16:2164–2175. https://doi.org/10.1105/tpc.104.023515

Ting CS, Hsieh C, Sundararaman S, Mannella C, Marko M (2007) Cryo-electron tomography reveals the comparative three-dimensional architecture of *Prochlorococcus*, a globally important marine cyanobacterium. J Bacteriol 189:4485–4493. https://doi.org/10.1128/JB.01948-06

Ulloa O, Canfield DE, DeLong EF, Letelier RM, Stewart FJ (2012) Microbial oceanography of anoxic oxygen minimum zones. Proc Natl Acad Sci USA 109:15996–16003. https://doi.org/10.1073/pnas.1205009109

Umena Y, Kawakami K, Shen JR, Kamiya N (2011) Crystal structure of oxygen-evolving photosystem II at a resolution of 1.9 A. Nature 473:55–60. https://doi.org/10.1038/nature09913

Veerman J, Bentley FK, Eaton Rye JJ, Mullineaux CW, Vasiliev S, Bruce D (2005) The PsbU subunit of photosystem II stabilizes energy transfer and primary photochemistry in the phycobilisome - Photosystem II assembly of *Synechocystis* sp PCC 6803. Biochemistry 44:16939–16948. https://doi.org/10.1021/bi051137a

Webb B, Sali A (2014) Protein structure modeling with MODELLER. In: Kihara D (ed) Protein structure prediction. Methods in molecular biology, vol 1137. Springer, New York, pp 1–15. https://doi.org/10.1007/978-1-4939-0366-5_1

Wegener KM, Bennewitz S, Oelmuller R, Pakrasi HB (2011) The Psb32 protein aids in repairing photodamaged photosystem II in the cyanobacterium *Synechocystis* 6803. Mol Plant 4:1052–1061. https://doi.org/10.1093/mp/ssr044

Welkie D, Zhang XH, Markillie ML, Taylor R, Orr G, Jacobs J, Bhide K, Thimmapuram J, Gritsenko M, Mitchell H, Smith RD, Sherman LA (2014) Transcriptomic and proteomic dynamics in the metabolism of a diazotrophic cyanobacterium, *Cyanothece* sp. PCC 7822 during a diurnal light-dark cycle. BMC Genom 15:1185. https://doi.org/10.1186/1471-2164-15-1185

Zinser ER, Lindell D, Johnson ZI, Futschik ME, Steglich C, Coleman ML, Wright MA, Rector T, Steen R, McNulty N, Thompson LR, Chisholm SW (2009) Choreography of the transcriptome, photophysiology, and cell cycle of a minimal photoautotroph, *Prochlorococcus*. PloS ONE 4:e5135. https://doi.org/10.1371/journal.pone.0005135

Zouni A, Witt HT, Kern J, Fromme P, Krauss N, Saenger W, Orth P (2001) Crystal structure of photosystem II from *Synechococcus elongatus* at 3.8 angstrom resolution. Nature 409:739–743. https://doi.org/10.1038/35055589

Affiliations

Frédéric Partensky[1,2] · Daniella Mella-Flores[1,2,3,4] · Christophe Six[1,2] · Laurence Garczarek[1,2] · Mirjam Czjzek[1,5] · Dominique Marie[1,2] · Eva Kotabová[6] · Kristina Felcmanová[6,7] · Ondřej Prášil[6,7]

1 Sorbonne Université, Station Biologique, CS 90074, 29688 Roscoff cedex, France

2 CNRS UMR 7144, Station Biologique, CS 90074, 29680 Roscoff, France

3 Facultad de Ciencias Biológicas, Pontificia Universidad Católica de Chile, Santiago, Chile

4 Center of Applied Ecology and Sustainability (CAPES-UC), Pontificia Universidad Católica de Chile, Santiago, Chile

5 CNRS UMR 8227, Marine Glycobiology Group, Station Biologique, CS 90074, 29680 Roscoff, France

6 Laboratory of Photosynthesis, Institute of Microbiology, MBU AVČR, Opatovický mlýn, 37981 Třeboň, Czech Republic

7 Faculty of Sciences, University of South Bohemia, Branišovská, 37005 České Budějovice, Czech Republic